Marine and Petroleum Geology 26 (2009) 1608–1623

Contents lists available at ScienceDirect

Marine and Petroleum Geology

journal homepage: www.elsevier.com/locate/marpetgeo

4D analogue modelling of transtensional pull-apart basins

Jonathan E. Wu [a,*], Ken McClay [a], Paul Whitehouse [a,1], Tim Dooley [b]

[a] Fault Dynamics Research Group, Department of Earth Sciences, Royal Holloway University of London, Egham, Surrey, TW20 OEX, UK
[b] Bureau of Economic Geology, Jackson School of Geosciences, The University of Texas at Austin, University Station, Box X, Austin, TX 78713-8924, USA

ARTICLE INFO

Article history:
Received 2 April 2008
Accepted 3 June 2008
Available online 3 July 2008

Keywords:
Pull-apart basins
Transtension
Pure strike-slip
Analogue modelling
En-echelon faults
Strain partitioning
Dead Sea
Vienna Basin

ABSTRACT

Scaled sandbox models were used to investigate the 4D evolution of pull-apart basins formed above underlapping releasing stepovers in both pure strike-slip and transtensional basement fault systems. Serial sectioning and 3D volume reconstruction permitted analysis of the full 3D fault geometries. Results show that very different pull-apart basins are developed in transtension compared to pure strike-slip. Both types of models produced elongate, sigmoidal to rhomboidal pull-apart systems, but the transtensional pull-apart basins were significantly wider and uniquely developed a basin margin of en-echelon oblique-extensional faults. Dual, opposing depocentres formed in the transtensional model whereas a single, central depocentre formed in pure strike-slip. In transtension, a distinct narrow graben system formed above the principal displacement zones (PDZs). Cross-basin fault systems that linked the offset PDZs formed earlier in the transtensional models.

Sequential model runs to higher PDZ displacements allowed the progressive evolution of the fault systems to be evaluated. In cross-section, transtensional pull-aparts initiated as asymmetric grabens bounded by planar oblique-extensional faults. With increasing displacement on the PDZs, basin subsidence caused these faults to become concave-upwards and lower in dip angle due to fault block collapse towards the interior of the basin. In addition, strain partitioning caused fault slip to become either predominantly extensional or strike-slip. The models compare closely with the geometries of natural pull-apart basins including the southern Dead Sea fault system and the Vienna Basin, Austria.

1. Introduction

Pull-apart basins are topographic depressions that form at releasing bends or steps in basement strike-slip fault systems. Traditional models of pull-apart basins usually show a rhombic to spindle-shaped depression developed between two parallel master vertical strike-slip fault segments, also known as principal displacement zones (PDZs). The basin is bounded longitudinally by a transverse system of oblique-extensional faults, termed "basin sidewall faults", that link with the bounding PDZs (e.g. Burchfiel and Stewart, 1966; Crowell, 1974; Mann et al., 1983; Christie-Blick and Biddle, 1985; Woodcock and Fischer, 1986; Sylvester, 1988; Mann, 2007).

The relative motion of the crustal blocks involved in a pull-apart system can either be parallel to the bounding PDZs (pure strike-slip) or oblique and divergent to the PDZs (transtensional). However, traditional models of pull-apart basins usually only consider the case of pure strike-slip motion (Fig. 1a) (e.g. Crowell, 1974; Mann et al., 1983; Christie-Blick and Biddle, 1985). Garfunkel (1981) proposes that significant changes occur when continental boundary strike-slip fault systems open with transtensional motion. Transtension introduces new surface area through the stretching of the plate edges, and fault slip partitions into pure strike-slip and transverse extensional components causing complex pull-apart basins to develop within a wide boundary zone. Three-dimensional elastic modelling by ten Brink et al. (1996) showed that a small component (5°) of transtension produces an area of subsidence 2–3 times wider at the surface compared to pure strike-slip. Accordingly, it is unclear whether pre-existing pull-apart basin models would also apply to transtensional pull-apart basins (Fig. 1b) and if not, how a transtensional pull-apart basin would evolve temporally and spatially.

Pull-apart basins that have developed with transtensional displacement on the PDZs are of significant economic importance and can contain giant hydrocarbon fields (e.g. Matzen Field, Vienna Basin; Fuchs and Hamilton, 2006), significant mineralisation (e.g. Escondida, Chile; Richards et al., 2001), and geothermal fields (e.g. Coso Geothermal Field, California; Monastero et al., 2005). They are usually zones of intense fracturing (e.g. Vienna Basin; Connolly and Cosgrove, 1999), elevated heat flow (Bohai Basin; Hu et al., 2001) and elevated seismicity (Marmara Sea; Armijo et al., 2002).

Scaled analogue modelling has proved to be a useful tool for simulating pull-apart basin geometries and evolution, with successful application to both pull-apart basins developed with

* Corresponding author. Tel.: +44 7977537529; fax: +44 1784 471780.
E-mail address: jonnyw@es.rhul.ac.uk (J.E. Wu).
[1] Current address: Hess, Level 9, The Adelphi Building, 1-11 John Adam Street, London, WC2N 6AG, UK.

0264-8172/$ – see front matter © 2008 Elsevier Ltd. All rights reserved.
doi:10.1016/j.marpetgeo.2008.06.007

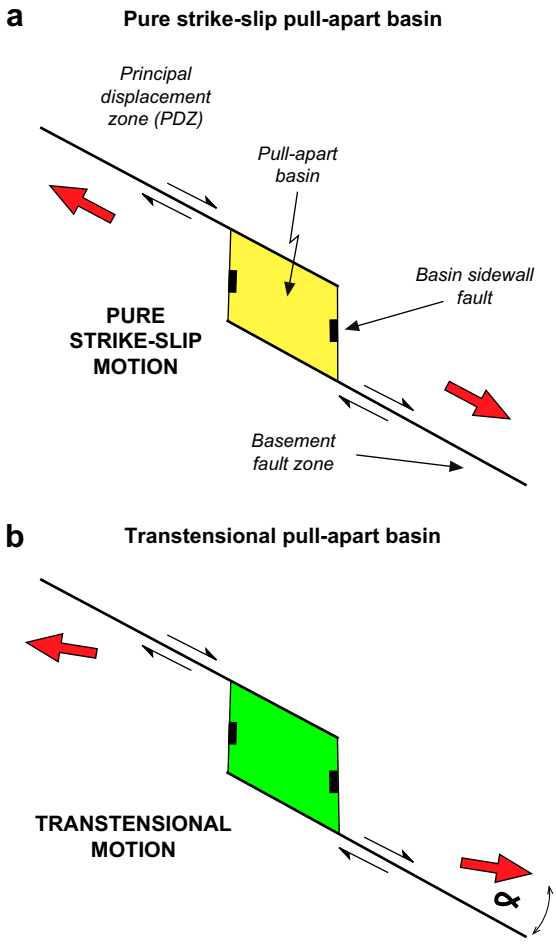

Fig. 1. General characteristics of a pull-apart basin in a dextral side-stepping fault system. The pull-apart basin is defined to develop in pure strike-slip when $\alpha = 0^\circ$ and in transtension when $0^\circ < \alpha \leq 45^\circ$.

displacement on the PDZs that is pure strike-slip (e.g. Hempton and Neher, 1986; Richard et al., 1995; Dooley and McClay, 1997; Rahe et al., 1998; Sims et al., 1999) and transtensional (Dooley et al., 2004).

This study compares scaled physical models of pull-apart basins developed with pure strike-slip and with transtensional motion along the PDZs. Subsequently, the 4D evolution of an analogue transtensional pull-apart basin is described using a suite of transtensional pull-apart models that have been serially sectioned at progressively greater levels of strike-slip displacement. Model results are compared to ancient and modern examples of transtensional pull-apart basins and a synoptic model for transtensional pull-apart basins is proposed.

2. Experimental procedure

To simulate a right-stepping dextral strike-slip fault system in rigid basement, aluminium plates were cut with a 30° underlapping releasing bend stepover geometry with a stepover width of 10 cm (Fig. 2). For pure strike-slip motion, the plates were displaced parallel to the trace of the PDZs and for transtensional motion, the plates were displaced at an angle of 5° oblique and divergent to the PDZs. During the experiments, the plates were displaced in opposing directions by stepper motors at an average rate of 2 cm/h.

In each experiment, a thin rubber membrane glued beneath the plates maintained extension across the PDZ and stepover and distributed strain across the plate boundaries. A spatially limited 1.5 cm-thick layer of 'SGM 36' polymer measuring 21 cm × 11 cm

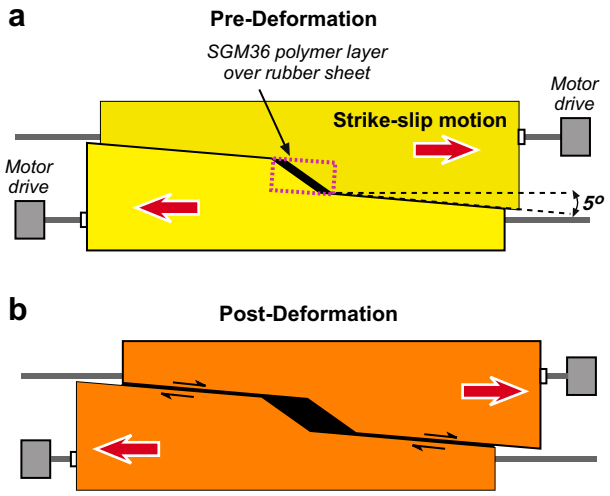

Fig. 2. Plan view of baseplate geometry used in transtensional pull-apart experiment.

was placed over the stepover to simulate a local rise in the brittle–ductile transition at depth, or the presence of a local viscous decollement. SGM 36, a Newtonian viscous material manufactured by Dow Corning Ltd., has a density of 965 kg m^{-3} with an effective viscosity of 5×10^4 Pa s at room temperature (20 °C). The use of SGM 36 in analogue modelling is well documented (Weijermars, 1986) and is analogous to a raised brittle–ductile transition in continental crust under a pull-apart basin (e.g. Petrunin and Sobolev, 2006; Monastero et al., 2005) or to a pre-kinematic sequence of brittle sedimentary rocks over a viscous decollement such as a salt layer (e.g. Al-Zoubi and ten Brink, 2001; Smit et al., 2008).

The dimensions of the sandpack in the rig were approximately 150 × 50 × 7.5 cm. Sand at the longitudinal margins of the model (parallel to strike-slip displacement direction) rested against fixed walls while sand at the transverse edge of the model was allowed to spill over freely at the angle of repose to minimize boundary effects. Dry quartz sand has an average angle of internal friction of 31°, a negligible cohesive strength (1.05 kPa) and deforms according to Navier–Coulomb failure, making it a favourable material for simulating the brittle deformation of sediments in the upper crust (e.g. Horsefield, 1977; McClay, 1990). The scaling of the model was set to a ratio of approximately 10^{-5}, such that 1 cm in the model represented approximately 1 km in nature.

The top surfaces of the models were photographed every 1 mm of strike-slip displacement and scanned with a laser every 2 mm of displacement according to methodologies described by Whitehouse (2005). Subsidence of the top surface was calculated from the incremental difference between successive gridded laser scans of the top surface.

In this paper, the results of six pull-apart experiments with identical starting conditions are described. The first experiment tested the development of a pull-apart basin with 6 cm of pure strike-slip displacement along the PDZs. Five experiments were then run with 5° transtensional displacement on the PDZs. These experiments were run to progressively greater transtensional displacements (2, 3, 4, 5 and 6 cm on the PDZs). In all models, syn-kinematic sedimentation was simulated by completely infilling the basin with a layer of red sand after 3 cm of strike-slip displacement and a layer of white sand after 5 cm of displacement. Completed models were impregnated with a gelling agent and serial vertical sections were sliced at 4 mm intervals and photographed. The photographs of the sections were reconstructed in 3D using Paradigm Geophysical's VoxelGeo software. Repeat experiments reproduced the results described in this study.

3. Experimental results

3.1. Plan view evolution: pure strike-slip

Fig. 3 illustrates the sequence of development that was observed in the pure strike-slip experiment using photographs and subsidence isopach maps generated from laser scanning of the surface of the model and fault interpretation, with the subsidence maps highlighting the differential subsidence between each photograph. During the initial phases of pull-apart formation (0–1.4 cm strike-slip displacement), left-stepping en-echelon dextral Riedel-shears (R-shears) propagated above the PDZs at an average

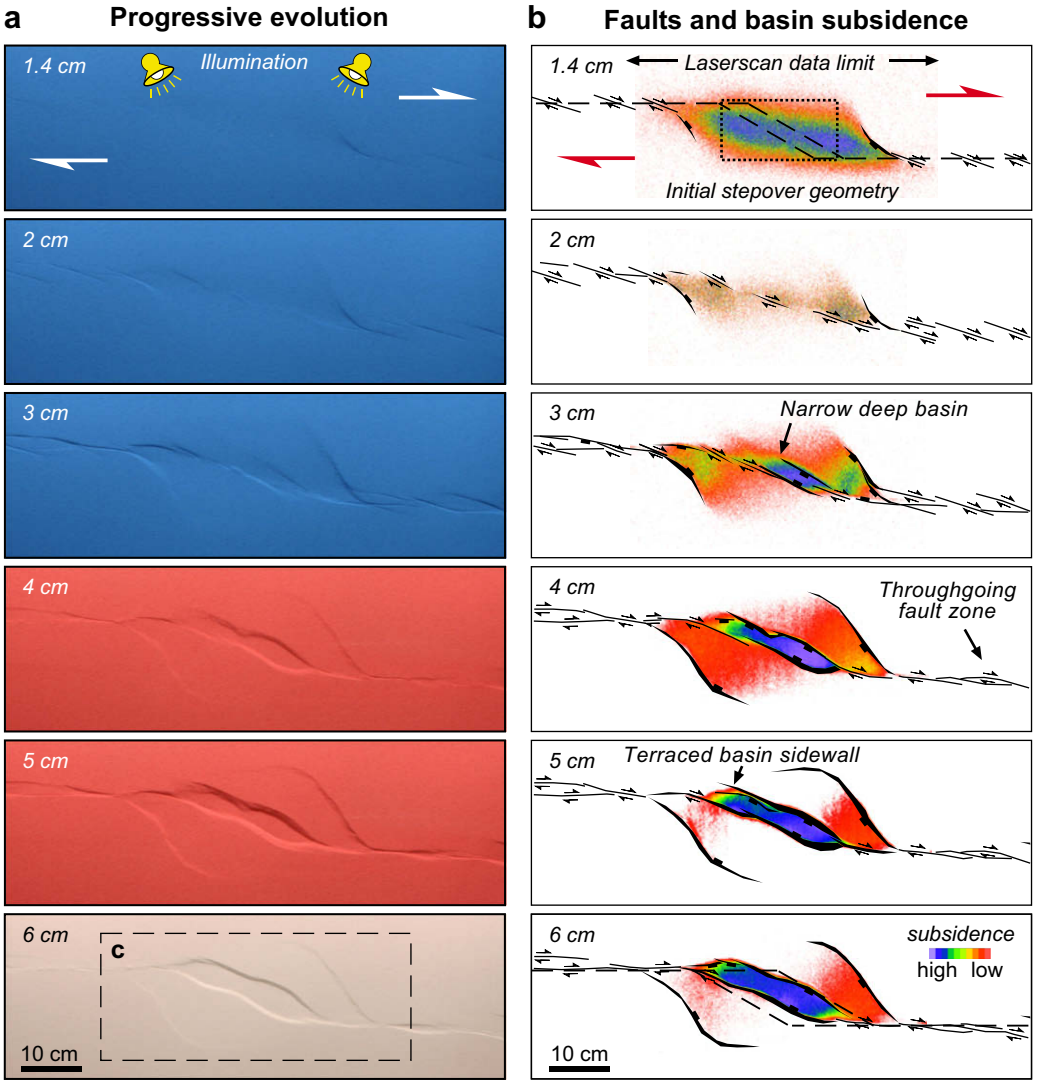

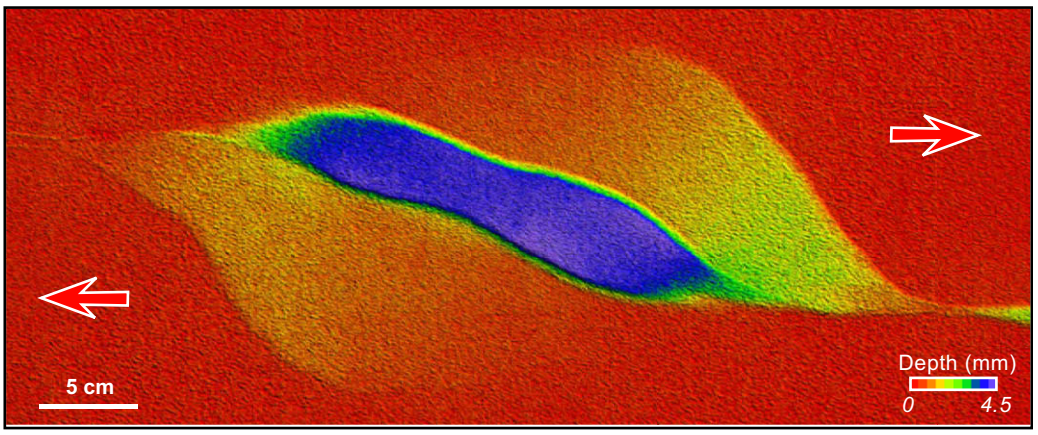

Fig. 3. Plan view evolution of pure strike-slip pull-apart basin model illustrated with: (a) time-lapse overhead photography; and (b) fault interpretation and incremental basin subsidence calculated from differential laser scans. Initial and final baseplate geometry shown with dashed lines; (c) basin topography at end of experiment.

strike of 22° clockwise to the trace of the PDZ in the basement. The R-shears linked with the first fault that formed above the stepover, which was an arcuate, oblique-extensional fault that bounded an elongate rhomboidal to sigmoidal-shaped area of subsidence.

At 2 cm of strike-slip displacement, the R-shears above the PDZs continued to propagate and lengthen. Synthetic P-shears propagated between the R-shears at a strike of 4° clockwise-oblique to the trace of the basement PDZs. Above the stepover, left-stepping dextral R-shears formed an en-echelon fault array across the stepover and subsidence continued.

With further strike-slip displacement (3–6 cm), the P-shears lengthened and linked with the R-shears to form a linear, narrow throughgoing fault zone composed of shear lenses above the PDZs. After the addition of syn-kinematic infill at 3 and 5 cm of strike-slip displacement, inactive faults were buried and only the active faults propagated upward through the infill. The oblique-extensional faults that originated from the intersection of the PDZs with the stepover continued to lengthen along an arcuate trace in plan view bounding subsidence of the hanging wall block. Above the stepover, long, oblique-extensional faults with opposite dip polarity propagated longitudinally with a strike of 27° clockwise to the trace of the PDZs, forming a flat-bottomed, deep, narrow and elongate rhomboidal-shaped basin comprised of two left-stepping linked grabens.

3.2. Plan view evolution: transtension

Fig. 4 shows the development of a pull-apart basin with 5° of transtensional displacement across the PDZs. The initial phase of pull-apart formation (0–1.4 cm transtensional displacement) produced left-stepping en-echelon dextral R-shears above the PDZs at an average strike of 16° clockwise to the trace of the PDZs in the basement. At the intersection of the PDZs with the stepover, an oblique-extensional fault developed that coalesced with the closest R-shear forming the longitudinal margins of subsidence. An elongate rhomboidal to sigmoidal-shaped area subsided to form depocentres within ellipsoidal zones at opposing ends of the stepover.

Between 2 and 3 cm of transtensional displacement, R-shears above the PDZs lengthened and synthetic P-shears initiated with a strike of 3° clockwise to the trace of PDZs. The R-shears and P-shears then began to slip with oblique extension while newly formed oblique-extensional faults propagated in-line with the borders of the PDZs. Above the stepover, a left-stepping en-echelon graben system formed that was bounded by en-echelon oblique-extensional fault segments striking at 28° clockwise to the trace of the PDZs. Dextral strike-slip fault segments propagated longitudinally across the centre of the basin. Subsidence continued above the stepover in dual opposing depocentres separated by an intra-basin high.

From 4 to 6 cm of transtensional displacement, oblique extension in the faults above the PDZs produced a narrow graben system in-line with the trace of the PDZs. The faults bounding the graben system strain-partitioned into left-stepping, segmented strike-slip faults opposite longer, oblique-extensional faults. This pattern was reversed longitudinally in the opposing PDZ. At the intersection of the stepover with the PDZs, an oblique-extensional fault continued to lengthen with an arcuate trace in plan view.

Above the stepover, left-stepping en-echelon oblique-extensional faults bounding the basin became soft-linked by relay ramp formation. With increasing displacement, these relay ramps were breached to form a basin sidewall fault composed of an irregular trace of hard-linked, left-stepping en-echelon faults. Syn-kinematic sedimentation, added after 5 cm of displacement, buried the inactive tips of the hard-linked en-echelon faults. Dextral strike-slip fault segments at the centre of the basin lengthened and linked, creating a cross-basin strike-slip fault zone connecting the partitioned strike-slip fault zones bordering the offset PDZs. In the latter stages, a component of dip-slip began on the cross-basin strike-slip fault.

The main area of subsidence gradually shifted from the basin centre to the southern half of the basin in an area bounded by the basin sidewall fault and the cross-basin strike-slip fault (5 and 6 cm models in Fig. 4). Finally, two new opposing depocentres formed within the new subsiding area.

3.3. Vertical sections: pure strike-slip model

Photographs of vertical serial sections were used to reconstruct isometric views of the internal geometry of the pure strike-slip model (Fig. 5a). Above the basement PDZs, a graben developed that was bounded by a simple, narrow, negative flower structure formed from a set of sub-vertical faults dipping at 65–90° (Sections A, B, F in Fig. 5a).

At the junction of the stepover with the PDZs, an asymmetric graben formed bounded by one sub-vertical (80–90° dip) concave-up fault and one shallow-dipping (35–65° dip) concave-up fault (e.g. Section E in Fig. 5a). These faults were linked longitudinally to fault zones above the PDZ and soled into the edge of the ductile decollement layer at depth (Sections C, E in Fig. 5a). The throw on some faults (e.g. Section C in Fig. 5a) decreased towards the base of the fault indicating, both dip- and strike-slip movement on the fault (e.g. oblique-extension). The fault blocks bounded by these faults tilted towards the sub-vertical faults (Section C, E in Fig. 5a). Above the centre of the basin, a deep and narrow graben formed that was bounded by a set of symmetric, upward-divergent, steeply dipping (70–80°) concave-up faults that soled into a reactive ridge of polymer at depth (Sections C, D, E in Fig. 5a). The maximum total thickness of the basin fill was 2.17 cm (Fig. 5a).

3.4. Vertical sections: transtensional model

Photographs of vertical serial sections were used to reconstruct the internal geometry of the transtensional model (Fig. 5b). Above the trace of the PDZs, a narrow graben formed that was bounded by an array of left-stepping sub-vertical faults. These faults had dips of 65–90° and formed a negative flower structure (Sections A, B, F in Fig. 5b). The throw on some faults (e.g. Section B in Fig. 5b) decreased towards the base of the fault, indicating both dip- and strike-slip on the fault (e.g. oblique-extension).

At the junction of the stepover with the PDZs, an asymmetric graben formed that was bounded on one side by a shallow-dipping (35–65°), concave-up fault that soled into the edge of the ductile decollement layer at depth. The opposite side of the graben showed a complex fault zone formed by a splay of upward-divergent fault segments with dips of 65–85° (Sections C, E in Fig. 5b). This fault zone corresponded to the en-echelon basin margin fault system in plan view. Above the centre of the basin, a central horst divided the basin into two symmetric graben bounded by sets of upward-divergent concave-up faults dipping 60–75° (Section D in Fig. 5b). The two graben were cross-cut by antithetic, steeply dipping to sub-vertical (77–90° dip) fault segments with a dip direction that flipped longitudinally across the basin (Section C, D in Fig. 5b). These antithetic faults formed the cross-basin strike-slip fault zone. The maximum thickness of the basin fill was 2.17 cm (Fig. 5b).

3.5. 3D visualisation

3D visualisations of the fault architecture from the model reconstructions show the differences between the models after 6 cm of strike-slip displacement. In the pure strike-slip model (Fig. 6a), a narrow negative flower structure characterises

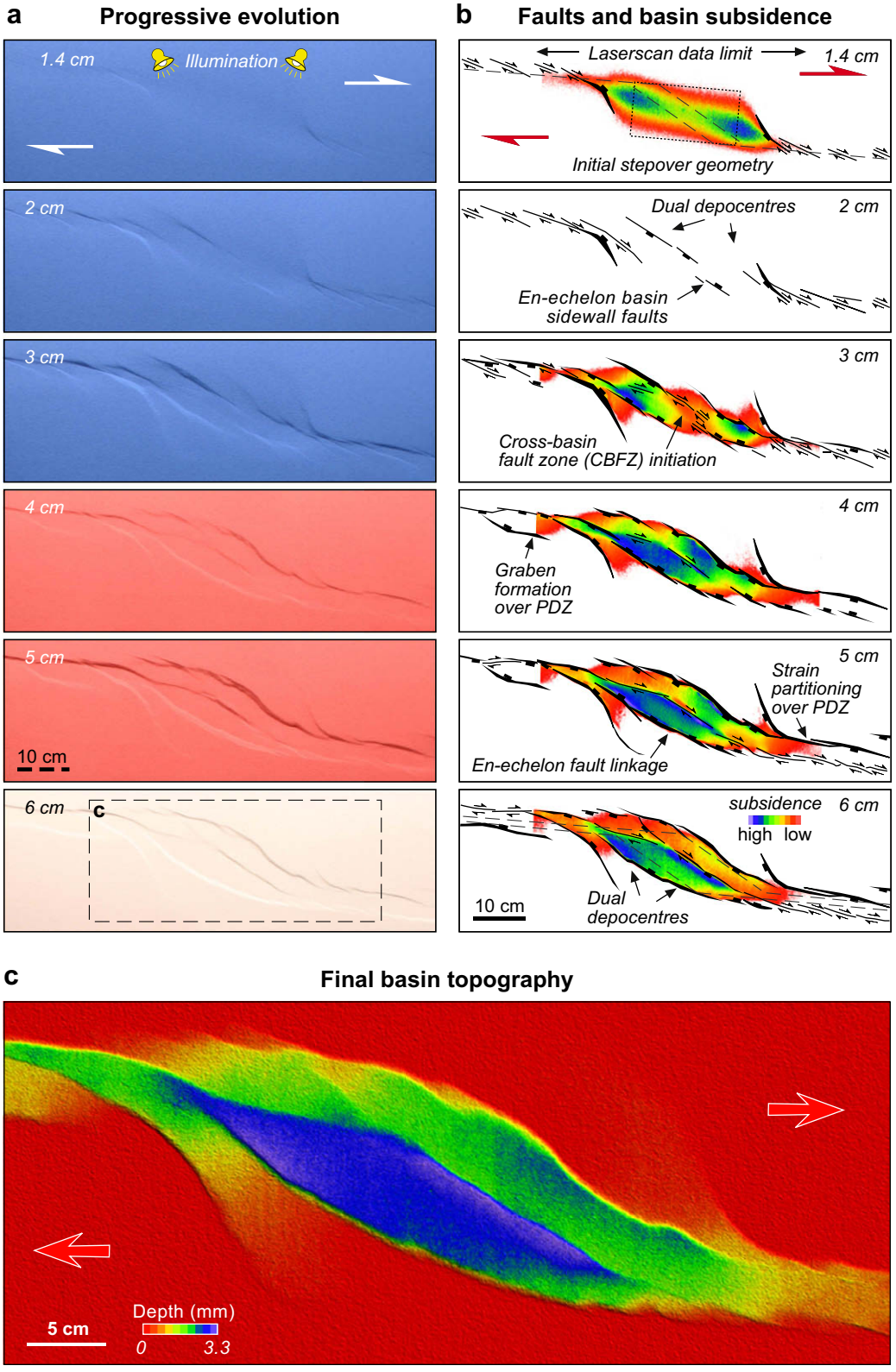

Fig. 4. Plan view evolution of transtensional pull-apart basin model illustrated with: (a) time-lapse overhead photography; and (b) fault interpretation and incremental basin subsidence calculated from differential laser scans. Initial and final baseplate geometry shown with dashed lines; (c) basin topography at end of experiment.

deformation above the PDZs. The central pull-apart basin above the basement stepover is composed of concave-upward faults that in plan view are curved in an elongate sigmoidal shape. Syn-kinematic sediments that infill the graben are sub-horizontal. At the margins of the basin, two concave-upward, shallow-dipping faults that are arcuate in plan view link longitudinally to the offset PDZs and sole at depth into the edge of the ductile decollement layer.

In the transtensional model (Fig. 6b), an array of left-stepping, upwardly divergent, and concave-upward helicoidal faults create a complex and broad negative flower structure above the PDZs. The

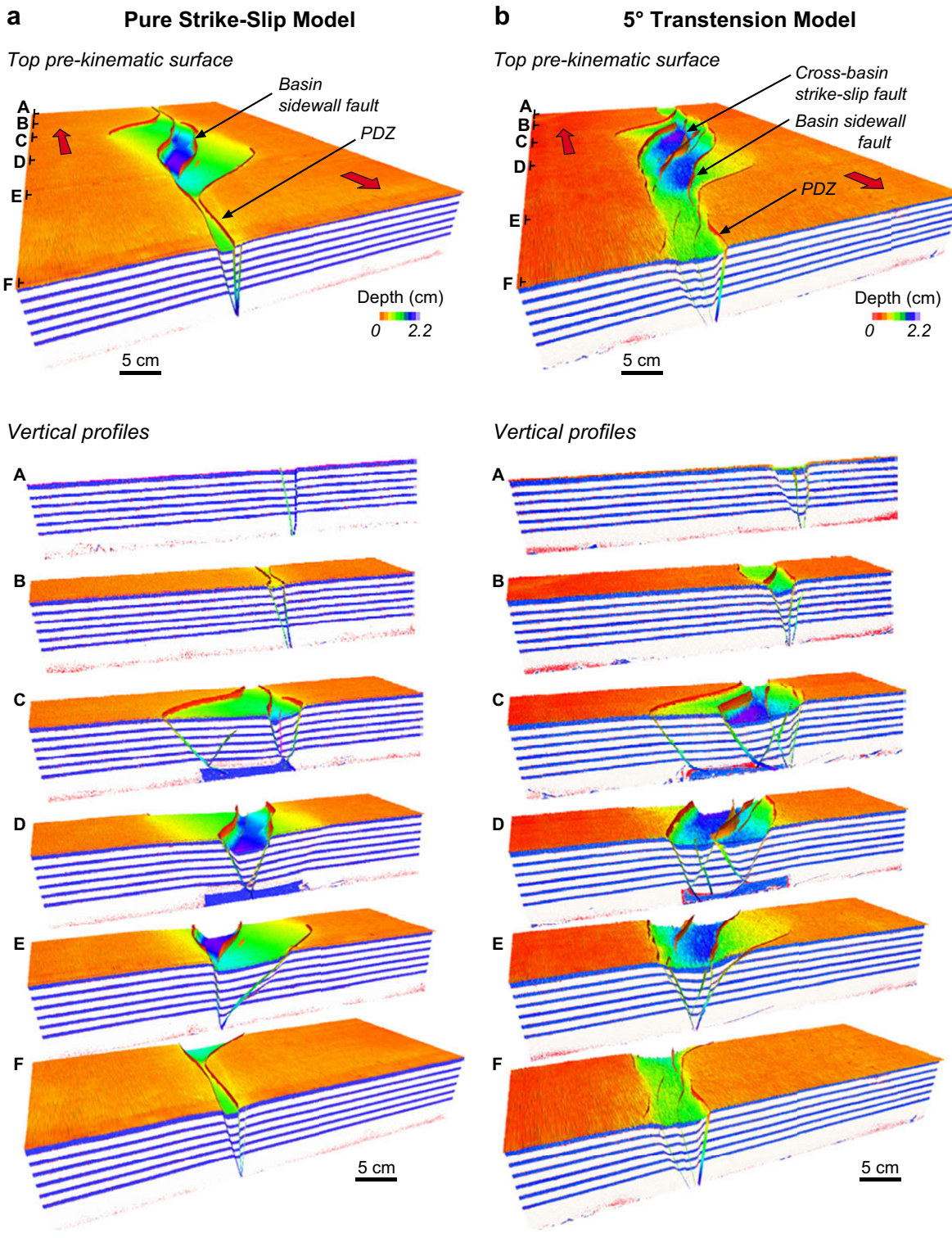

Fig. 5. 3D visualisation of pull-apart basin model reconstructions. (a) Pure strike-slip model; and (b) transtensional model. The top surface is the top of the pre-kinematic sequence.

basin sidewalls consist of concave-upward faults that curve into an elongate sigmoidal to rhomboidal shape in plan view. The basin interior is cut by a cross-basin strike-slip zone that consists of an array of conjugate sub-vertical, helicoidal faults linking the offset PDZs. An intra-basin horst block, bounded by the cross-basin fault system, forms a relative high in the centre of the basin. The syn-kinematic fill is sub-horizontal and infills fault-bounded depocentres.

3.6. 4D evolution of transtensional model

Sequential model runs to increasing displacements on the PDZs allowed examination of the progressive evolution of the models. After 2 cm of transtensional displacement (Fig. 7a), faults initiated as upwardly divergent, steeply dipping to sub-vertical planar faults. Basin-bounding faults above the basin margin (B–B′ and D–D′ in

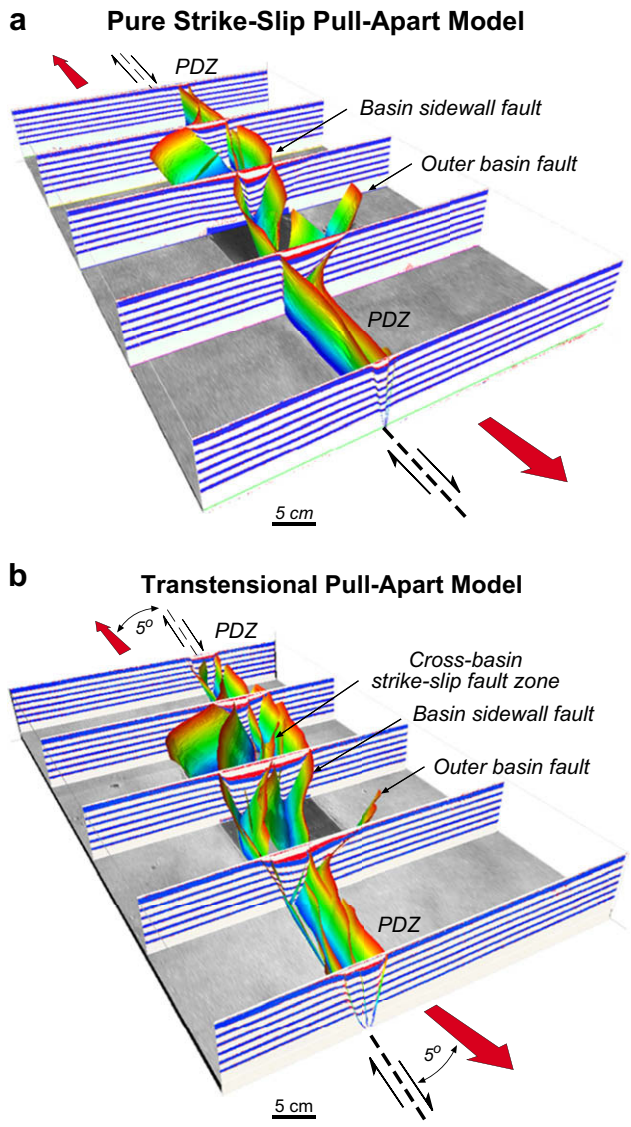

Fig. 6. 3D visualisation of fault architectures of pull-apart basin models developed in: (a) pure strike-slip; and (b) transtension.

Fig. 7a) formed an asymmetric graben that reversed its symmetry longitudinally across the basin. Basin-bounding faults over the centre of the basin (C–C′ in Fig. 7a) were symmetric.

With increasing transtensional displacement (3–6 cm models in Fig. 7a), the initially planar faults became concave-upwards and lowered in dip angle. At the basin margins, new steeply dipping to sub-vertical faults initiated in the centre of graben system. Thickening of the syn-kinematic strata shows that these new faults, accommodated most of the basin subsidence as displacement on the PDZs increased (B–B′ and D–D′ in 5 and 6 cm models in Fig. 7a). In the basin centre, the steeply dipping faults of the cross-basin strike-slip system initiated both antithetic and synthetic to the basin-bounding faults (C–C′ in 5 and 6 cm models of Fig. 7a).

Fig. 8 shows 3D fault reconstructions from transtensional pull-apart analogue models with 2, 4 and 6 cm of strike-slip displacement on the PDZs. After 2 cm of transtensional displacement (Fig. 8a), both the faults above the PDZs and through the centre of the stepover were planar and steep to sub-vertically dipping (70–90°), while the faults at the basin margins were planar and shallower dipping (60–70°). At 4 cm displacement (Fig. 8b), faults over the PDZs remained steep to sub-vertically dipping (70–90°) but began to take on a curved concave-up, helicoidal shape in 3D. Faults above the stepover became concave-up, helicoidal and lower in dip angle (60–80°). At 6 cm displacement (Fig. 8c), faults above the PDZs remained steep to sub-vertically dipping (70–90°). The dip angles of both the basin bounding faults and the cross basin fault zone faults became lower, at 50–70° and 60–80°, respectively.

4. Discussion

4.1. A comparison of pure strike-slip and transtensional pull-apart basin geometries

Overall, both pure strike-slip and transtensional models produced broadly similar elongate rhomboidal to sigmoidal basins with arcuate oblique-extensional sidewall faults in plan view (Figs. 3 and 4). This geometry is similar to many active and ancient pull-apart basins (e.g. Crowell, 1974; Mann et al., 1983; Aydin and Nur, 1985; Christie-Blick and Biddle, 1985; Mann, 2007) and previous physical models of pull-apart basins (e.g. Hempton and Neher, 1986; Dooley and McClay, 1997; Rahe et al., 1998; Sims et al., 1999; Dooley et al., 2004).

The elongate shape of our pull-apart basins can be attributed to the use of a basal ductile decollement similar to Sims et al. (1999). Models using purely brittle materials without a basal ductile decollement (e.g. Dooley and McClay, 1997; Rahe et al., 1998) still produce rhomboidal to sigmoidal-shaped basins but are less elongate. An identical set of "outer basin faults" (Fig. 6a, b) nucleated at the lateral edge of the basal decollement layer in both models. The location and presence of these faults is a result of the use of a laterally confined basal ductile layer in the experiment design, but similar faulting can be expected in natural systems if an abrupt lateral termination of a ductile layer at depth exists. In the models presented in this study, the dip direction of the master fault switched longitudinally across the basin (Fig. 5a, b). This longitudinal symmetry resulted from the equal rate of strike-slip displacement between the basement plates. Longitudinally asymmetric pull-apart basins would be expected when the opposing sides of the basin move with unequal rates of strike-slip motion (Rahe et al., 1998; Basile and Brun, 1999), or with only one moving plate (Rahe et al., 1998; Smit et al., 2008).

Despite the broad similarities, the minor change in plate motion from pure strike-slip to 5° transtensional displacement across the PDZs introduced distinct changes in the structural style and intrabasinal geometry of the models. The maximum depth of the two basins, equal to the maximum thickness of the syn-kinematic fill layers, was the same (2.17 cm) (Fig. 5a, b). However, the transverse limit of the main central basin in the transtensional model (calculated using the distance between the 'basin sidewall faults' in Fig. 6a, b) was up to 3 times wider than that of the pure strike-slip model (Figs. 3c and 4c).

The sidewall faults of the pure strike-slip basin were formed from a single oblique-extensional fault that was long and arcuate in plan view (6 cm model in Fig. 3b). In contrast, the sidewall faults of the transtensional pull-apart basin were formed by segmented, left-stepping en-echelon oblique-extensional faults (3 cm model in Fig. 4b) that hard- and soft-linked to form an irregular, arcuate surficial fault trace (5 cm model in Fig. 4b) with increasing transtensional displacement. The pure strike-slip pull-apart basin developed a single central depocentre (3 cm model in Figs. 3b and 5a) while the transtensional model developed dual depocentres at opposite ends of the basin that were separated by a relative structural high (3 cm model in Figs. 4b and 5b). Above the PDZs, the pure strike-slip model developed a narrow, throughgoing fault zone of shear lenses (6 cm model in Fig. 3b). The transtensional model developed a distinct narrow graben system bounded on

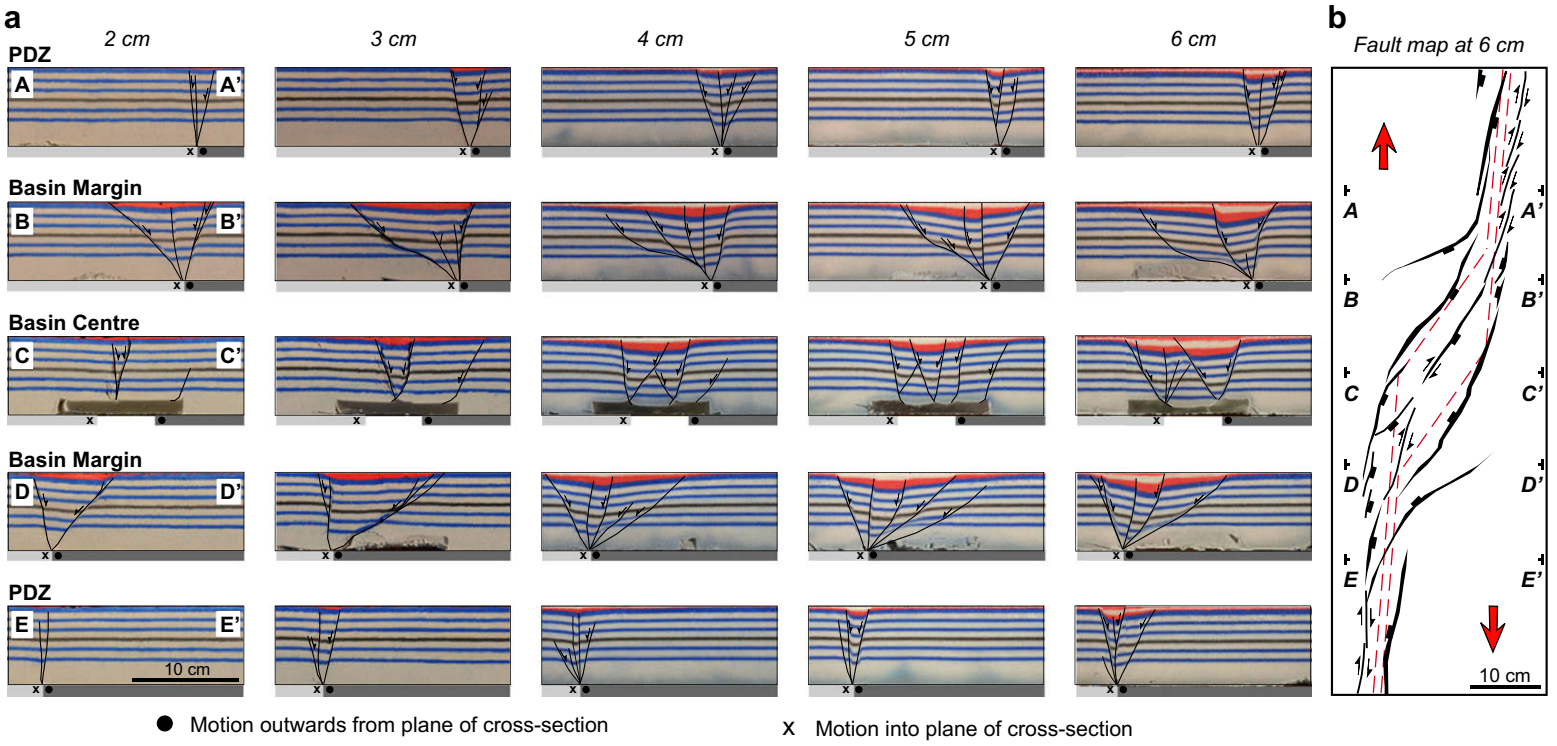

Fig. 7. Synoptic compilation showing the 4D evolution of a pull-apart basin in transtension. (a) Vertical sections with fault interpretation for five locations in a series of transtensional pull-apart analogue models with progressively greater strike-slip displacement (2, 3, 4, 5, and 6 cm). (b) Fault map from 6 cm model showing section locations.

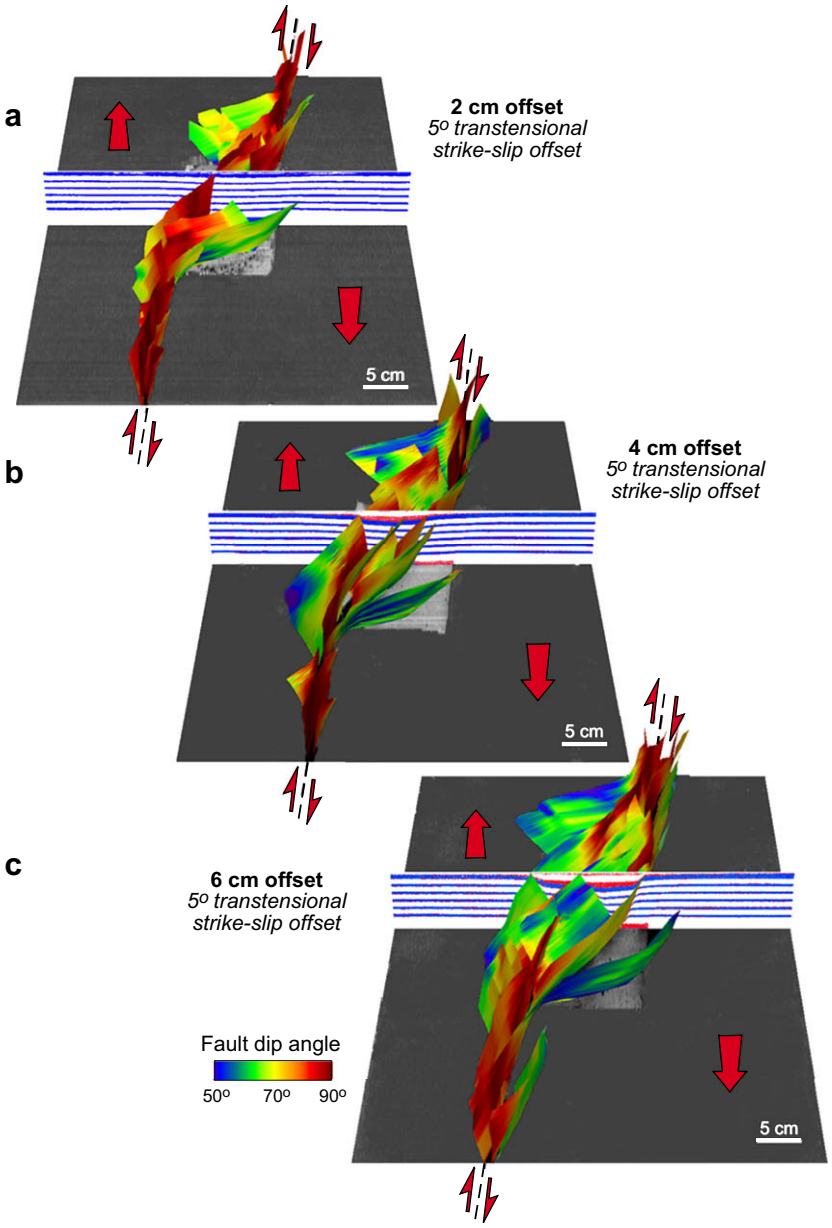

Fig. 8. 4D fault evolution shown through a comparison of 3D fault reconstructions of transtensional pull-apart models with: (a) 2 cm; (b) 4 cm; and (c) 6 cm of dextral 5° transtensional displacement on the PDZs.

opposite sides by sets of en-echelon dextral strike-slip faults and oblique-extensional faults that formed in-line with the borders of the PDZ (6 cm model in Fig. 4b). In the latter stages of the transtensional experiment, a cross-basin strike-slip fault zone formed that linked the offset PDZs (Fig. 4b) while no cross-basin fault zone was developed in the pure strike-slip model.

A disproportionately large increase in width (3 times) of the main, inner pull-apart basin was caused by the introduction of a small component (5°) of oblique divergent slip between the PDZs. These results are consistent with results of 3D elastic modelling of parallel overlapping strike-slip faults by ten Brink et al. (1996), in which 5° of transtensional slip produced an area of subsidence that was 2–3 times wider at the surface compared to an equivalent pure strike-slip model. In transtension, small increases in oblique fault motion add a large component of region subsidence compared to pure strike-slip. The increased area of surficial subsidence in our models was the result of the oblique and divergent movement of the basin sidewalls. The footwalls of the sidewall faults, which are pinned to the basement, move away from the hanging wall. This causes the hanging wall to collapse downwards (Fig. 7) and the dip angles of faults to lower (Fig. 8). Subsidence is accommodated in the cover by upward-diverging fault sets that formed negative flower structures (e.g. Fig. 7). The Marlborough fault system, New Zealand, contains an example of an array of pull-apart in which some of the basins are developed in dextral pure strike-slip and some in transtension due to changes in the orientation of the Hope fault relative to the regional plate motions (de Mets et al., 1990). A comparison of the pure strike-slip Poplars and GlynnWye pull-apart basins (Clayton, 1966; Freund, 1971; Cowan, 1990) with the transtensional Hanmer pull-apart basin (Wood et al., 1994) shows that the transtensional Hanmer basin is clearly longer (20 km compared to 2.5 km) and wider (10 km compared to 1 km) than the pure strike-slip basins. The increase in size between the two types of basin along the Marlborough fault system are likely to be at least

partially influenced by the change from pure strike-slip to transtension, but may also be the result of other factors such as differences in the initial stepover geometry or the depth to the basement.

An en-echelon marginal fault system composed of overlapping oblique-extensional faults uniquely developed in our transtensional pull-apart models (Figs. 3c and 4c). In physical (e.g. Hempton and Neher, 1986; Dooley and McClay, 1997; Rahe et al., 1998; Sims et al., 1999; this study) and numerical (e.g. ten Brink et al., 1996) models of pure strike-slip pull-apart basins, en-echelon marginal fault systems do not develop. Instead, these basin margins develop as a single or terraced margin of sub-parallel, oblique-extensional faults. En-echelon faulted margins develop similarly in analogue models of highly oblique rift systems (e.g. Tron and Brun, 1991; Schreurs and Colleta, 1998; McClay et al., 2002; Gutowski and Koyi, 2007). It is therefore proposed that an en-echelon marginal fault system in a pull-apart basin is a primary indicator that the basin has developed with oblique and divergent (e.g. transtensional) motion.

A natural example of a transtensional pull-apart basin with this structural style is the Vienna Basin, Austria (Fig. 9). The Vienna Basin is a thin-skinned pull-apart basin that developed on the basal detachment of the Alpine–Carpathian orogenic wedge in a left overstep of a major sinistral transform system between the Eastern Alps and the Western Carpathians. The basin initiated in the Miocene and was later subjected to compressional inversion in the Pliocene (Royden, 1985; Sauer et al., 1992; Fodor, 1995; Decker, 1996; Horvath and Clotingh, 1996). A map of the Vienna Basin (Fig. 9a) shows that the basin sidewalls are dominated by en-echelon oblique-extensional faults (e.g. Royden, 1985; Hinsch et al., 2005a,b; Arzmuller et al., 2006) similar to the model results in this study (3 and 4 cm models, Fig. 4).

In cross-section (Fig. 9b), this en-echelon basin margin system appears as a negative flower structure bounded by an upward-divergent splay of faults. This cross-sectional fault geometry is similar to our transtensional model results (e.g. B–B′ in 3 cm model in Fig. 7a) with the exception that some faults in Fig. 9b have a slight reversal of throw that is likely the result of the Pliocene inversion event. The asymmetry of the graben in Fig. 9b, together with progressively changing dips of the basin fill, suggests an asymmetric tilting of the graben. This fault asymmetry is reversed at the opposite longitudinal margin of the basin (Arzmuller et al., 2006). These features compare well to those developed near the longitudinal basin margins in our models (e.g. B–B′ and D–D′ in Fig. 7a) and to previous pull-apart models (e.g. Dooley and McClay, 1997).

Other natural examples of transtensional pull-apart basin systems with en-echelon marginal fault systems include the Coso Wash in California (e.g. Monastero et al., 2005; Pluhar et al., 2006), the Central Basin of the Marmara Sea, Turkey (e.g. Armijo et al., 2002), and the Milne Point pull-apart basin, Alaska (Casavant et al., 2004). The en-echelon basin margin fault systems in our transtensional models formed soft-linked relays that breached with increasing strain to become a long, hard-linked zigzag fault trace. In the Pannonian Basin, central Hungary, field observations of hard-linked relay ramps between en-echelon faults in a transtensional setting (Fodor, 2007) show that they are oblique-extensional or pure-extensional faults that strike oblique to the main en-echelon fault segments.

One of the most striking features in our transtensional models was the development of dual depocentres separated by an intra-basin structural high (3 cm model in Figs. 4b and 5b). This feature is not unique to physical models of transtensional systems (Dooley et al., 2004, 2007) and has been produced in models of pure strike-slip pull-apart basins above a ductile decollement (Sims et al., 1999). Numerical models of pure strike-slip pull-apart basins (e.g. Rodgers, 1980; Gölke et al., 1994; Katzman et al., 1995) also develop this feature. This depocentre geometry develops because the area

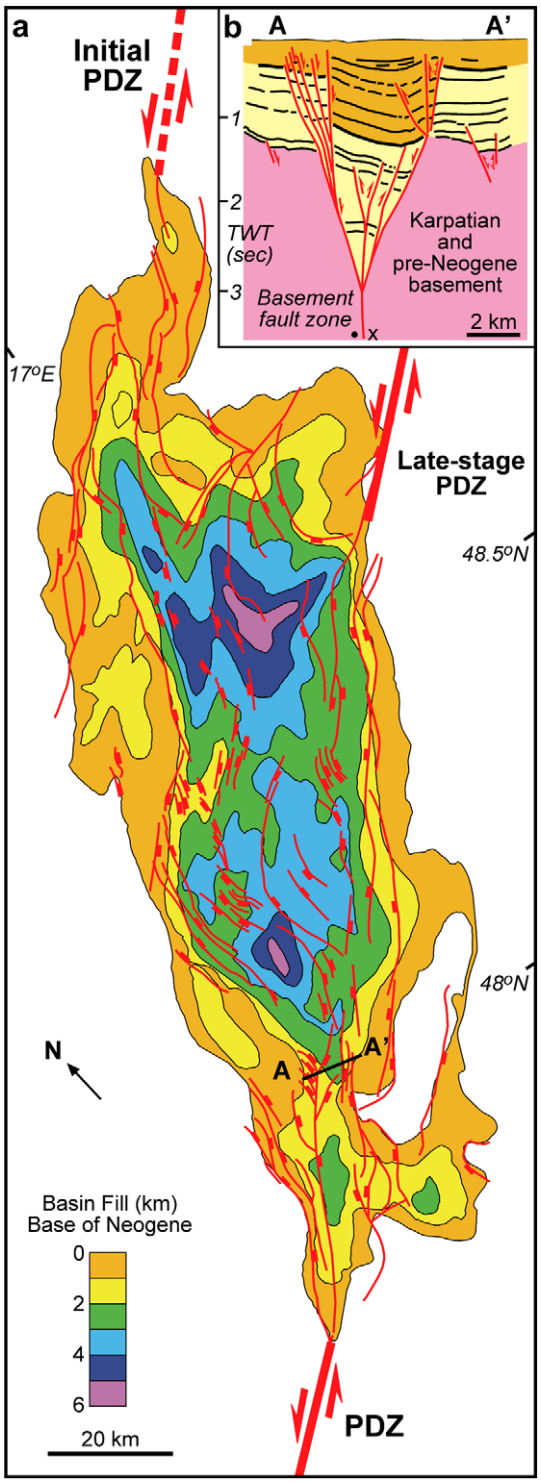

Fig. 9. (a) Summary map of faults and basin fill of the Vienna Basin (modified from Hinsch et al., 2005a; Arzmuller et al., 2006) showing en-echelon faulting along the basin margins and the development of dual depocentres. (b) Cross-section re-interpreted from seismic in Hinsch et al. (2005a) shows an asymmetric negative flower structure bounded by a splay of en-echelon faults.

of maximum extension in both pure strike-slip and transtensional pull-apart basins occurs at the junction of the PDZs with the stepover (Bertoluzza and Perotti, 1997). In addition, the development of discrete depocentres within a pull-apart basin system can be the result of an underlying weak layer (Sims et al., 1999) and not due to plate motions. Nevertheless, our experiments show that the

development of a dual depocentre system should be greatly enhanced in a transtensional pull-apart basin (compare 3 cm models in Figs. 3b and 4b). Natural examples of transtensional pull-apart basins such as the Vienna Basin in Austria (Fig. 9) (e.g. Fodor, 1995; Arzmuller et al., 2006), the Ghab Basin of the northern Dead Sea Fault System (Brew et al., 2001), and the Cariaco basin, Venezuela (Schubert, 1982) exhibit a well-developed dual depocentre geometry separated by a relative high block that is comparable to our transtensional models.

A cross-basin strike-slip fault zone forms to allow faults to straighten and 'shortcut' across strike-slip releasing bends as they widen (e.g. Wesnousky, 1988; Zhang and Burchfiel, 1989; McClay and Dooley, 1995). Because our transtensional pull-apart basin model widened significantly faster than the pure strike-slip model with equivalent PDZ displacement (compare Figs. 3c and 4c), it follows that cross-basin strike-slip fault systems should be better developed in transtensional pull-apart basins. This effect is seen in our experiments where after 6 cm of PDZ displacement a cross-basin strike-slip fault system was developed only in the transtensional model (Figs. 3c and 4c). However, the development of this fault system is not unique to either pure strike-slip or transtensional pull-apart systems and has been observed in analogue models of both pure strike-slip (Dooley and McClay, 1997; Rahe et al., 1998) and transtensional pull-aparts (Dooley et al., 2004, 2007, this study). Sims et al. (1999) postulated that throughgoing cross-basin strike-slip fault systems are not well developed in pull-apart systems with weak decollements, but the results of this study show that a cross-basin fault system will develop even above weak decollements when a pull-apart basin system has sufficiently widened. De Paola et al. (2007) hypothesized from field observations that the formation of a cross-basin strike-slip fault is inhibited in transtensional pull-aparts because fault patterns are disrupted as the failure mode changes from shear to tensile failure with increasing strain. Natural examples of transtensional pull-apart

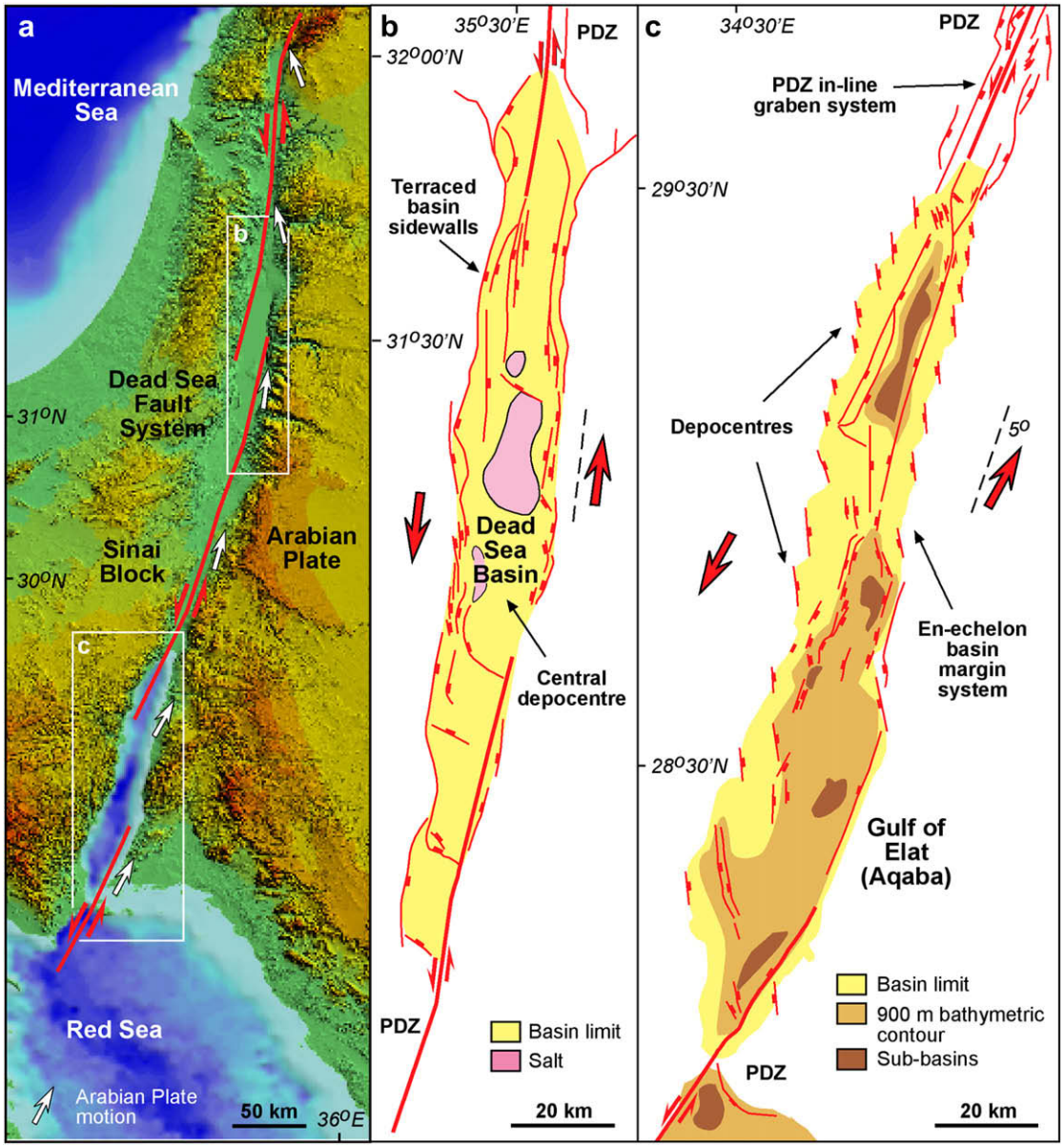

Fig. 10. Pull-apart systems in the southern end of the Dead Sea fault system. (a) SRTM digital elevation model topography showing plate motion model derived from GPS geodesy (Reilinger et al., 2006), the location of the pure strike-slip Dead Sea Basin pull-apart basin in the north and the transtensional Gulf of Elat (Aqaba) pull-apart basin in the south; (b) Structural interpretation map of the Dead Sea Basin pull-apart (Garfunkel and Ben-Avraham, 1996); (c) Structural interpretation map of the Gulf of Aqaba pull-apart (modified from Ben-Avraham et al., 1979; Ben-Avraham, 1985; Ehrhardt et al., 2005).

basins suggest that a variety of outcomes may occur. In the Cariaco Basin, Venezuela, a cross-basin strike-slip fault system developed through the straightening of the Moron-El Pilar Fault, causing pull-apart extinction (Jaimes-Carvajal and Mann, 2003). In the Vienna Basin, Austria (Fig. 9a), continued strike-slip motion caused extinction of one PDZ and strike-slip motion to transfer through a linear transfer fault zone across the remaining PDZ (Hinsch et al., 2005a; Decker et al., 2005).

4.2. A comparison of basins in the southern Dead Sea fault system

The southern end of the well-studied sinistral Dead Sea fault system (DSFS) (e.g. Quennell, 1958; Freund et al., 1970; Garfunkel, 1981) allows for a comparison of natural pull-apart basins formed in pure strike-slip and in transtensional settings (Fig. 10). The DSFS is estimated to have accumulated approximately 105 km of sinistral slip (Quennell, 1959; Freund, 1965; Freund et al., 1970). 60–70 km of sinistral slip occurred in the Mid-Late Miocene and the remainder of sinistral slip occurred in a second phase from the Early Pliocene to present day, during which time a number of pull-apart basins along the southern DSFS are thought to have formed simultaneously (Freund et al., 1970). Tectonic reconstructions show that during the latest phase of slip, the southern portion of the DSFS, including the Gulf of Aqaba (Elat), began to move with 2–5° transtension. In contrast, further north at the location of the Dead Sea Basin, the plate motion was pure strike-slip (Garfunkel, 1981). Recent GPS geodetic studies (Reilinger et al., 2006; Mahmoud et al., 2005; Wdowinski et al., 2004) confirm that these plate motions continue to the present day.

The differences in geometry and structural style between the transtensional Gulf of Aqaba pull-apart basin (Fig. 10c) and the pure strike-slip Dead Sea pull-apart basin (Fig. 10b) compare well with our analogue model results. The Gulf of Aqaba basin is slightly wider (28 km compared to 20 km maximum width) and longer

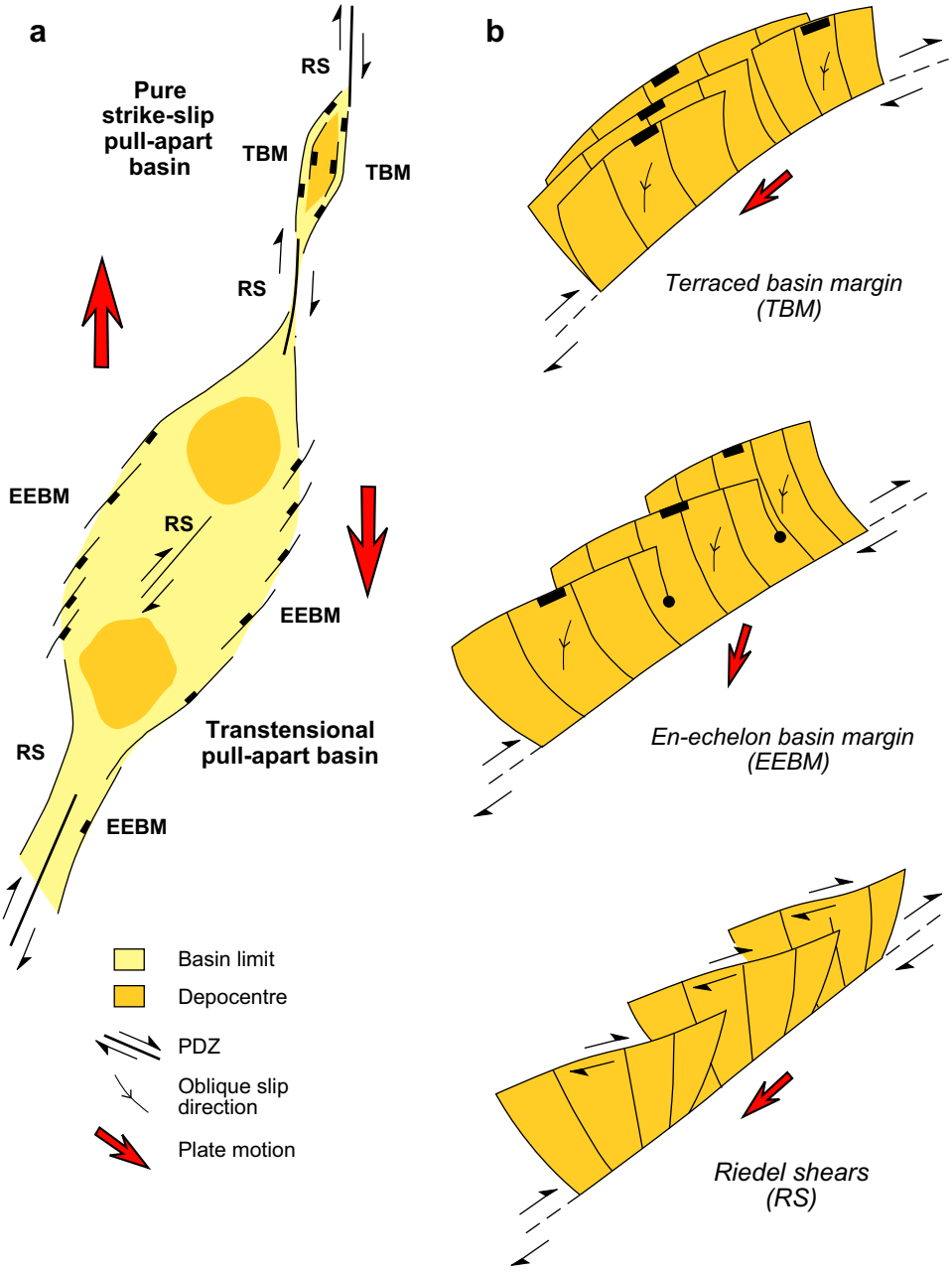

Fig. 11. (a) Plan view location of fault styles in a dextral pure strike-slip (top) and transtensional (bottom) pull-apart basin system. (b) 3D geometries of fault styles.

than the Dead Sea Basin (180 km compared to 150 km) (Ben-Avraham, 1985; Garfunkel and Ben-Avraham, 1996). The margins of the Gulf of Aqaba are dominated by NNW-trending, right-stepping en-echelon extensional faults that have linked to form a distinct zigzag pattern (Ben-Avraham et al., 1979). In contrast, the Dead Sea Basin has a terraced basin margin with sub-parallel oblique-extensional faults (ten Brink and Ben-Avraham, 1989). Within the Gulf of Aqaba, major depocentres have formed at opposite ends of the pull-apart basin while the Dead Sea Basin contains one central depocentre bounded longitudinally by strike-slip fault segments. Bathymetric and seismic data from the northern Gulf of Aqaba show that the northern margin is bounded by an asymmetric graben system with tilted growth strata (Ben-Avraham et al., 1979; Ehrhardt et al., 2005). Although these differences compare well with our models, some of the contrasts in geometry between the two basins are also undoubtedly controlled by other factors. For example, the basement geometry of the Gulf of Aqaba is unlikely to be as simple as our models and may actually reflect a composite pull-apart system.

The northern extension of the Gulf of Aqaba, a 5-km wide graben system bounded by oblique-extensional faults, may represent the in-line graben system developed above the PDZs in our transtensional models (e.g. Section F in Fig. 5b). Recent mapping using gravity (ten Brink et al., 1999) and remote sensing (Kesten et al., 2008) of this area reveals a string of long and narrow buried basins offset en-echelon by shorter (25–55 km), discontinuous fault segments. In contrast, the PDZs at the northern and southern boundaries of the Dead Sea are narrower and predominantly zones of strike-slip. One major difference to our models is that the main depocentre of the Dead Sea Basin migrated northwards with increasing strike-slip on the PDZs (ten Brink and Ben-Avraham, 1989). In our pure strike-slip model, the central depocentre basin deepened but did not migrate because its location was fixed by the baseplate geometry.

Fig. 11a shows a comparison of structural styles developed in an idealised system with both a pure strike-slip pull-apart basin and a transtensional pull-apart basin, based on the model results and comparisons with natural examples. The main distinction is the formation of a terraced basin margin (Fig. 11b) in a pure strike-slip pull-apart system and a soft- or hard-linked en-echelon basin margin system (Fig. 11c) in a transtensional pull-apart system. The en-echelon basin margin fault style should not be confused with Riedel-shears (Fig. 11d), which also have an en-echelon surface trace and appear in both systems. A secondary distinction is that the depocentre in a pure strike-slip pull-apart basin will generally be at the basin centre while in transtension, significant depocentres are expected to develop at opposite ends of the basin (Fig. 11a). Fig. 12 illustrates a 3D synoptic model of an idealised, early stage, transtensional pull-apart basin based on the results of this study.

4.3. 4D evolution of transtensional pull-apart basins

In our models, increasing strain caused faults to partition into families of predominantly oblique-extensional and strike-slip faults. Above the stepover, separation of slip into a discrete cross-basin strike-slip zone and a separate set of en-echelon oblique-extensional sidewall faults (3–6 cm models in Fig. 4b) can be understood as a consequence of strain partitioning. In addition, faults above the PDZs partitioned into one set of Riedel-shears and an opposing set of oblique-extensional faults (5–6 cm models in

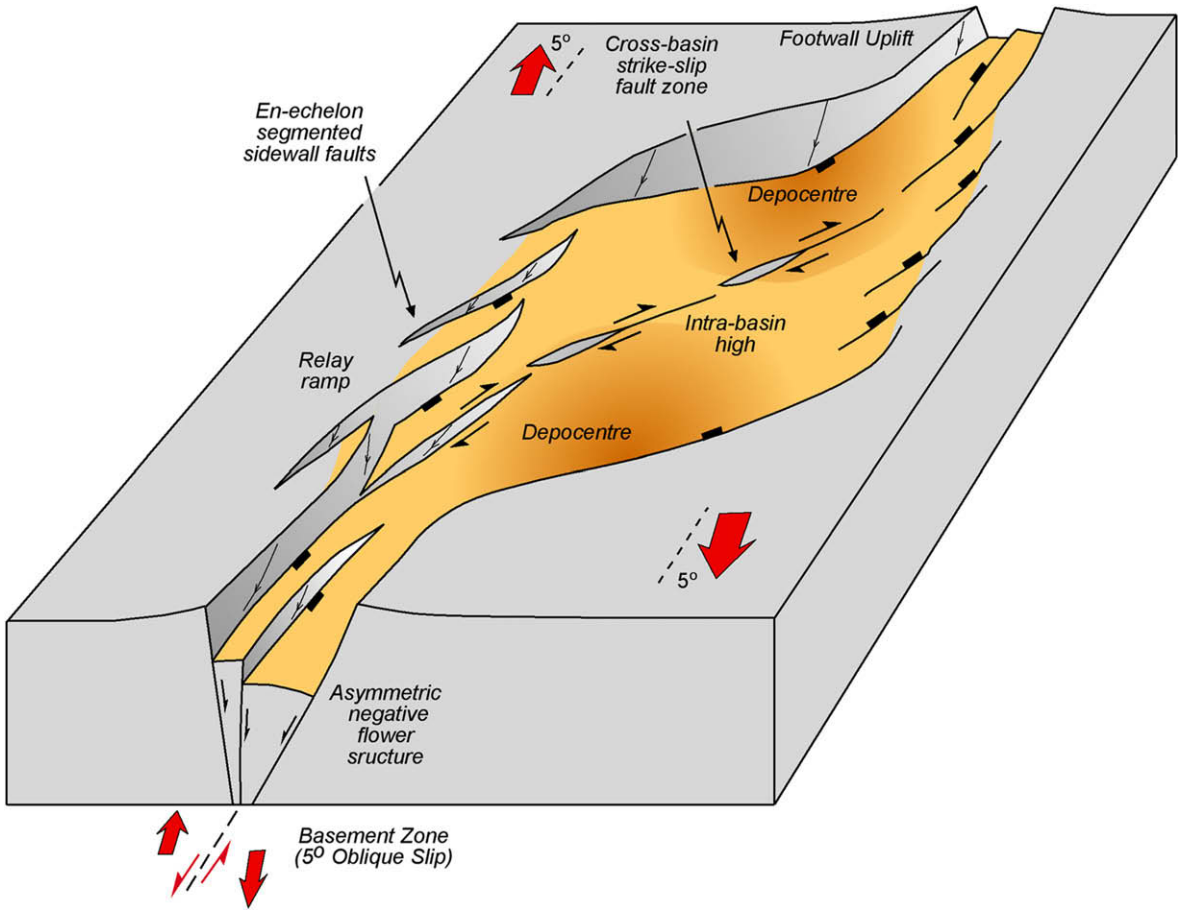

Fig. 12. Three-dimensional geometry of an idealised early stage pull-apart basin developing in 5° transtension based on the results of analogue modelling.

Fig. 4b). Strain partitioning is characteristic of oblique-slip systems and can be explained by the upward elastoplastic propagation of a localized basement fault or shear zone at depth (Bowman et al., 2003). Bowman et al. (2003) showed that the static stress field above a pure strike-slip fault at depth is a simple strike-slip stress field, while a buried oblique-slip fault tip propagating from depth separates into an arrangement of discrete zones of normal, reverse and strike-slip faulting. King et al. (2005) demonstrated from the 2001 Kokoxili earthquake in China that strain partitioning occurs in nature even when motion along a strike-slip fault is as little as 2–3° obliquely divergent (transtensional) to the master fault. Strain partitioning is observed in the present day in the Vienna Basin (Fig. 9) where fault movement within the mature transtensional pull-apart structure occurs as separate domains of predominantly strike-slip and predominantly normal faulting (Hinsch et al., 2005b).

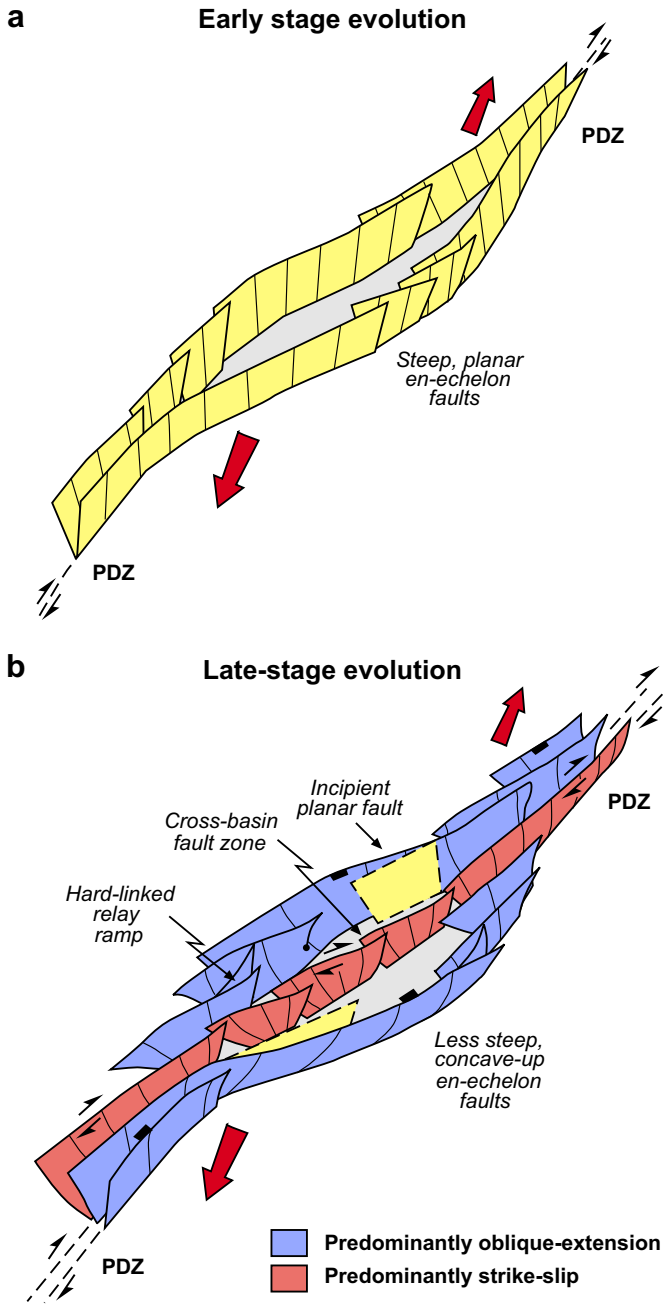

Fig. 13. 4D fault evolution of a transtensional pull-apart basin system. (a) Early stage of evolution with a narrow basin formed between planar sub-vertical en-echelon faults. (b) Late-stage of evolution with soft- and hard-linked concave-upward en-echelon faults and initiation of new planar faults. Strain partitioning causes faults to become predominantly extensional or strike-slip.

The fault population in the models showed a progressive lowering of fault dip, a change from planar to listric fault geometries and the collapse of fault blocks into the stepover with increasing displacement on the PDZs (Figs. 7a and 8). These patterns were noted in 4D analyses of analogue and numerical models of extension above a ductile decollement using X-rays (Schreurs et al., 2006; Buiter et al., 2006). The patterns in our models cannot be attributed to the effects of syn-kinematic sedimentation as they were observed during both phases of sediment-starvation (2–3 cm models in Fig. 7a) and sedimentation (4–6 cm models in Fig. 7a). 4D changes in the fault profiles from planar to listric are the result of faults decoupling from the basement due to the basal rubber/polymer decollement above the basement stepover, while the lowering of fault dips is due to the collapse of footwall blocks into the stepover as the hanging wall of the basin sidewall faults, which are pinned to basement, move outwards. With increasing displacement on the PDZs, subsidence generated above the stepover caused faults to curve concave-upward as they soled into the ductile decollement layer at depth (Fig. 13). As the structure widens and collapses inwards, new steeper-dipping planar faults are initiated with geometries similar to the first-formed faults (compare active faults of B–B′ in 2 and 6 cm models in Fig. 7a).

5. Conclusions

Scaled analogue modelling of pull-apart basins developed above underlapping, releasing stepovers shows that very different basins are developed in transtensional (oblique divergent) slip along the basement master fault zones compared to pure strike-slip. In both settings the gross geometry consists of elongate, sigmoidal to rhomboidal, pull-apart basins. However, in transtension the pull-apart basin margin is characterized by the development of en-echelon oblique-extensional faults that soft- or hard-link with increasing displacement on the PDZs. En-echelon faulting is not observed at the basin margins of the pure strike-slip model, which instead develops a basin margin composed of terraced, sub-parallel oblique-extensional faults. Therefore, an en-echelon basin margin system is an important primary indication that a pull-apart basin has likely developed in transtension.

Basin size and subsidence patterns are also influenced by a change from pure strike-slip to transtension. The introduction of a small amount of oblique divergent slip (5° transtension) causes the main central basin of the models to be disproportionately wider (2–3 times). A “dual opposing depocentre” geometry develops in the early to middle stages of transtensional basin evolution. This geometry, where depocentres at opposite ends of the stepover were separated by an intra-basin relative high block, was different to the pure strike-slip model which had a single central depocentre. While a significantly greater basin width and the development of a “dual opposing depocentre” geometry are not unique to transtensional pull-apart basins, they can be used as secondary indicators that a pull-apart basin is developing in transtension.

Digital reconstructions of sequential model runs to higher displacements on the PDZs allowed the progressive evolution of transtensional pull-apart systems to be evaluated. In cross-section, transtensional pull-aparts models initiate as asymmetric grabens bounded by planar faults. Increased PDZ displacement causes faults to become concave-upwards and decrease in dip angle as fault blocks collapse into the stepover. In addition, the faults strain-partition into domains of predominantly dip-slip or strike-slip faults. Cross-basin fault systems that link the offset PDZs form much earlier in the transtensional basin due to an increased rate of basin widening.

The general fault and basin geometries of our analogue models compare favourably to natural pull-apart basins. Within the Dead Sea fault system, the differences in depocentre location and fault geometries of the pure strike-slip Dead Sea Basin and the transtensional Gulf of Aqaba (Elat) basin systems compare well to our respective pure strike-slip and transtensional models. The Vienna Basin, Austria, demonstrates that the basin margins of natural pull-apart basins in transtension are also dominated by en-echelon oblique-extensional faulting and often develop dual depocentres separated by an intra-basinal high.

Acknowledgements

We thank Frank Monastero and the US Navy Geothermal Program Office for supporting the modelling project with the Fault Dynamics Research Group, Royal Holloway University of London, UK. We are grateful to Rob Bond and Paradigm Geophysical for contributing VoxelGeo software and jointly developing the model reconstructions. Bob Casavant of the University of Arizona is thanked for discussions about the Milne Point Basin, Alaska. Mike Craker is thanked for building the lab apparatus and Kevin D'Souza for help with photography and logistics. Simon Craggs is thanked for reviewing earlier versions of this manuscript.

References

Al-Zoubi, A., ten Brink, U.S., 2001. Salt diapirs in the Dead Sea basin and their relationship to Quaternary extensional tectonics. Marine and Petroleum Geology 18, 779–797.

Armijo, R., Meyer, B., Navarro, S., King, G., Barka, A., 2002. Asymmetric slip partitioning in the Sea of Marmara pull-apart: a clue to propagation processes of the North Anatolian Fault? Terra Nova 14 (2), 80–86.

Arzmuller, G., Buchta, S., Ralbovsky, E., Wessely, G., 2006. The Vienna Basin. In: Golonka, J., Picha, F.J. (Eds.), The Carpathians and Their Foreland: Geology and Hydrocarbon Resources. AAPG Memoir 84, 191–204 (Chapter 5).

Aydin, A., Nur, A., 1985. The types and roles of stepovers in strike slip tectonics. In: Biddle, K.T., Christie-Blick, N. (Eds.), Strike-slip Deformation, Basin Formation, and Sedimentation. Society of Economic Paleontologists and Mineralogists, Special Publication, vol. 37, pp. 35–45.

Basile, C., Brun, J.P., 1999. Transtensional faulting patterns ranging from pull apart basins to transform continental margins; an experimental investigation. Journal of Structural Geology 21, 23–37.

Ben-Avraham, Z., 1985. Structural framework of the gulf of Elat (Aqaba), northern Red Sea. Journal of Geophysical Research 90, 703–726.

Ben-Avraham, Z., Almagor, G., Garfunkel, Z., 1979. Sediments and structure of the gulf of Elat (Aqaba) – Northern Red Sea. Sedimentary Geology 23, 239–267.

Bertoluzza, L., Perotti, C.R., 1997. A finite-element model of the stress field in strike-slip basins: implications for the Permian tectonics of the Southern Alps (Italy). Tectonophysics 280, 185–197.

Bowman, D., King, G., Tapponnier, P., 2003. Slip partitioning by elastoplastic propagation of oblique slip at depth. Science 300, 1121–1123.

Brew, G., Lupa, J., Barazangi, M., Sawaf, T., Al-Imam, A., Zaza, T., 2001. Structure and tectonic development of the Ghab basin and the Dead Sea fault system, Syria. Journal of the Geological Society, London 158, 665–674.

Buiter, S.J.H., Babeyko, A.Y., Ellis, S., Gerya, T.A., Kaus, B.J.P., Kellner, A., Schreurs, G., Yamada, Y., 2006. The numerical sandbox: comparison of model results for a shortening and an extension experiment. In: Buiter, S.J.H., Schreurs, G. (Eds.), Analogue and Numerical Modelling of Crustal-Scale Processes. Geological Society of London, Special Publication, vol. 253, pp. 29–64.

Burchfiel, B.C., Stewart, J.H., 1966. Pull-apart origin of the central segment of Death Valley, California. Geological Society of America Bulletin 77, 439–442.

ten Brink, U.S., Ben-Avraham, Z., 1989. The anatomy of a pull-apart basin; seismic reflection observations of the Dead Sea Basin. Tectonics 8, 333–350.

ten Brink, U.S., Katzman, R., Lin, j., 1996. Three-dimensional models of deformation near strike-slip faults. Journal of Geophysical Research 101 (B7), 16025–16220.

ten Brink, U.S., Rybakov, M., Al-Zoubi, A.S., Hassouneh, M., Frieslander, U., Batayneh, A.T., Goldschmidt, V., Daoud, M.N., Rotstein, Y., Hall, J.K., 1999. Anatomy of the Dead Sea transform: does it reflect continuous changes in plate motion? Geology 27 (10), 887–890.

Casavant, R., Hennes, A., Johnson, R., Collett, T., 2004. Structural analysis of a proposed pull-apart basin: implications for gas hydrate and associated free-gas emplacement, Milne Point Unit, Arctic Alaska. In: AAPG Hedberg Conference, "Gas Hydrates: Energy Resource Potential and Associated Geologic Hazards", Vancouver, BC, Canada.

Christie-Blick, N., Biddle, K.T., 1985. Deformation and basin formation along strike-slip faults. In: Biddle, K.T., Christie-Blick, N. (Eds.), Strike-slip Deformation, Basin Formation, and Sedimentation. Society of Economic Paleontologists and Mineralogists, Special Publication, vol. 37, pp. 1–35.

Clayton, L., 1966. Tectonic depressions along the Hope fault, a transcurrent fault in North Canterbury, New Zealand. New Zealand Journal of Geology and Geophysics 9, 95–104.

Cowan, H.A., 1990. Late Quaternary displacements on the Hope Fault at Glynn Wye, North Canterbury. New Zealand Journal of Geology and Geophysics 33, 285–293.

Connolly, P., Cosgrove, J., 1999. Prediction of fracture-induced permeability and fluid flow in the crust using experimental stress data. AAPG Bulletin 83 (5), 757–777.

Crowell, J.C., 1974. Sedimentation along the San Andreas fault, California. In: Dott, R.H., Shaver, R.H. (Eds.), Modern and Ancient Geosynclinal Sedimentation. Society of Economic Paleontologists and Mineralogists Special Paper, vol. 19, pp. 292–303.

Decker, K., 1996. Miocene tectonics at the Alpine–Carpathian junction and the evolution of the Vienna Basin. Mitteilungen der Gesellschaft der Geologie und Bergbaustudenten in Ö sterreich 41, 33–44.

Decker, K., Peresson, H., Hinsch, R., 2005. Active tectonics and Quaternary basin formation along the Vienna Basin Transfer fault. Quaternary Science Reviews 24, 305–320.

de Mets, C., Gordon, R.G., Argus, D.F., Stein, S., 1990. Current plate motions. Geophysical Journal International 101, 425–478.

De Paola, N., Holdsworth, R.E., Collettini, C., McCaffrey, K.J.W., Barchi, M.R., 2007. The structural evolution of dilational stepovers in regional transtensional zones. In: Cunningham, W.D., Mann, P. (Eds.), Tectonics of Strike-slip Restraining and Releasing Bends. Geological Society of London, Special Publications, vol. 290, pp. 433–446.

Dooley, T., McClay, K.R., 1997. Analog modeling of pull-apart basins. AAPG Bulletin 81, 1804–1826.

Dooley, T., Monastero, F., Hall, B., McClay, K.R., Whitehouse, P., 2004. Scaled sandbox modelling of transtensional pull-apart basins: applications to the Coso geothermal system. Geothermal Research Council Transactions 28, 637–641.

Dooley, T., Monastero, F.C., McClay, K.R., 2007. Effects of a weak crustal layer in a transtensional pull-apart basin: results from a scaled physical modeling study. Eos 88, Abstract V53F–04.

Ehrhardt, A., Hubscher, C., Ben-Avraham, Z., Gajewski, D., 2005. Seismic study of pull-apart-induced sedimentation and deformation in the Northern Gulf of Aqaba (Elat). Tectonophysics 396, 59–79.

Fodor, L.I., 1995. From transpression to transtension: Oligocene–Miocene structural evolution of the Vienna basin and the East Alpine-Western Carpathian junction. Tectonophysics 242, 151–182.

Fodor, L.I., 2007. Segment linkage and the state of stress in transtensional transfer zones: field examples from the Pannonian Basin. In: Cunningham, W.D., Mann, P. (Eds.), Tectonics of Strike-slip Restraining and Releasing Bends. Geological Society of London, Special Publications, vol. 290, pp. 417–432.

Freund, R., 1965. A model of the structural development of Israel and adjacent areas since Upper Cretaceous times. Geology Magazine 102, 189–205.

Freund, R., 1971. The Hope Fault: a strike-slip fault in New Zealand. New Zealand Geological Survey Bulletin 86, 1–49.

Freund, R., Garfunkel, Z., Zak, I., Goldberg, M., Weissbrod, T., Derin, B., 1970. The shear along the Dead Sea rift. Philosophical Transactions of the Royal Society of London, Series A 267, 107–130.

Fuchs, R., Hamilton, W., 2006. New depositional architecture for an old giant: the Matzen Field, Austria. In: Golonka, J., Picha, F.J. (Eds.), The Carpathians and Their Foreland: Geology and Hydrocarbon Resources. AAPG Memoir 84, 205–219 (Chapter 6).

Garfunkel, Z., 1981. Internal structure of the Dead Sea leaky transform (rift) in relation to plate kinematics. Tectonophysics 80, 81–108.

Garfunkel, Z., Ben-Avraham, Z., 1996. The structure of the Dead Sea. Tectonophysics 266, 155–176.

Gölke, M., Cloetingh, S., Fuchs, K., 1994. Finite-element modeling of pull-apart basin formation. Tectonophysics 240, 45–57.

Gutowski, J., Koyi, H.A., 2007. Influence of oblique basement strike-slip faults on the Mesozoic evolution of the south-eastern segment of the Mid-Polish Trough. Basin Research 19, 67–86.

Hempton, M., Neher, K., 1986. Experimental fracture, strain and subsidence patterns over en-echelon strike-slip faults: implications for the structural evolution of pull-apart basins. Journal of Structural Geology 8, 597–605.

Hinsch, R., Decker, K., Peresson, H., 2005a. 3-D seismic interpretation and structural modeling in the Vienna Basin: implications for Miocene to recent kinematics. Austrian Journal of Earth Sciences 97, 38–50.

Hinsch, R., Decker, K., Wagreich, M., 2005b. 3-D mapping of segmented active faults in the southern Vienna Basin. Quaternary Science Reviews 24, 321–336.

Horsefield, W.T., 1977. An experimental approach to basement-controlled faulting. Geologie en Mijnbouw 56, 363–370.

Horvath, F., Clotingh, S., 1996. Stress-induced late-stage subsidence anomalies in the Pannonian Basin. Tectonophysics 266, 287–300.

Hu, S., O'Sullivan, P.B., Raza, A., Kohn, B.P., 2001. Thermal history and tectonic subsidence of the Bohai Basin, northern China: a Cenozoic rifted and local pull-apart basin. Physics of the Earth and Planetary Interiors 126 (3), 221–235.

Jaimes-Carvajal, M., Mann, P., 2003. Tectonic origin of the Cariaco basin, Venezuela: Pull-apart, extinct pull-apart, or fault-normal extension? In: AAPG Annual Meeting, Salt Lake City, Utah, May 11–14, 2003.

Katzman, R., ten Brink, U.S., Lin, J., 1995. Three-dimensional modelling of pull-apart basins: implications for the tectonics of the Dead Sea Basins. Journal of Geophysical Research 100 (B4), 6295–6312.

Kesten, D., Weber, M., Haberland, Ch., Janssen, Ch., Agnon, A., Bartov, Y., Rabba, I., 2008. Combining satellite and seismic images to analyse the shallow structure of the Dead Sea Transform near the DESERT transect. International Journal of Earth Science 97 (1), 153–169.

King, G., Klinger, Y., Bowman, D., Tapponnier, P., 2005. Slip-Partitioned Surface Breaks for the Mw 7.8 2001 Kokoxili Earthquake, China. Bulletin of the Seismological Society of America 95 (2), 731–738.

Mahmoud, S., Reilinger, R., McClusky, S., Vernant, P., Tealeb, A., 2005. GPS evidence for northward motion of the Sinai block: implications for E. Mediterranean tectonics. Earth and Planetary Science Letters 238, 217–224.

Mann, P., 2007. Global catalogue, classification and tectonic origins of restraining- and releasing bends on active and ancient strike-slip fault systems. In: Cunningham, W.D., Mann, P. (Eds.), Tectonics of Strike-slip Restraining and Releasing Bends. Geological Society of London, Special Publications, vol. 290, pp. 13–142.

Mann, P., Hempton, M.R., Bradley, D.C., Burke, K., 1983. Development of pull-apart basins. Journal of Geology 91, 529–554.

McClay, K.R., 1990. Deformation mechanics in analogue models of extensional fault systems. In: Knipe, R.J., Rutter, E.H. (Eds.), Deformation Mechanisms, Rheology and Tectonics. Geological Society of London, Special Publications, vol. 54, pp. 445–453.

McClay, K.R., Dooley, T., 1995. Analogue models of pull-apart basins. Geology 23, 711–714.

McClay, K.R., Dooley, T., Whitehouse, P., Mills, M., 2002. 4-D evolution of rift systems: insights from scaled physical models. AAPG Bulletin 86, 935–960.

Monastero, F.C., Katzenstein, A.M., Miller, J.S., Unruh, J.R., Adams, M.C., Richards-Dinger, K., 2005. The Coso geothermal field: a nascent metamorphic core complex. Bulletin of the Geological Society of America 117, 1534–1553.

Petrunin, A., Sobolev, S.V., 2006. What controls thickness of sediments and lithospheric deformation at a pull-apart basin? Geology 34 (5), 389–392.

Pluhar, C.J., Coe, R.S., Lewis, J.C., Monastero, F.C., Glen, J.M.G., 2006. Fault block kinematics at a releasing stepover of the Eastern California shear zone: partitioning of rotation style in and around the Coso geothermal area and nascent metamorphic core complex. Earth and Planetary Science Letters 250 (1–2), 134–163.

Quennell, A.M., 1958. The structural and geomorphic evolution of the Dead Sea rift. Quarterly Journal of the Geological Society of London 114, 1–24.

Quennell, A.M., 1959. Tectonics of the Dead Sea rift. In: Proceedings of the 20th International Geological Congress, Mexico, pp. 385–403.

Rahe, B., Ferrill, D., Morris, A., 1998. Physical analog modeling of pull-apart basin evolution. Tectonophysics 285, 21–40.

Reilinger, R., McClusky, S., Vernant, P., Lawrence, S., Ergintav, S., Cakmak, R., Ozener, H., Kadirov, F., Guliev, I., Stepanyan, R., Nadariya, M., Hahubia, G., Mahmoud, S., Sakr, K., ArRajehi, A., Paradissis, D., Al-Aydrus, A., Prilepin, M., Guseva, T., Evren, E., Dmitrotsa, A., Filikov, S.V., Gomez, F., Al-Ghazzi, R., Karam, G., 2006. GPS constraints on continental deformation in the Africa–Arabia–Eurasia continental collision zone and implications for the dynamics of plate interactions. Journal of Geophysical Research – Solid Earth 111, B5.

Richard, P.D., Naylor, M.A., Koopman, A., 1995. Experimental models of strike-slip tectonics. Petroleum Geoscience 1, 71–80.

Richards, J.P., Boyce, A.J., Pringle, M.S., 2001. Geologic evolution of the Escondida area, northern Chile: a model for spatial and temporal localization of porphyry Cu mineralization. Economic Geology 96 (2), 271–305.

Rodgers, D.A., 1980. Analysis of pull-apart basin development produced by en-echelon strike-slip faults. In: Ballance, P., Reading, H. (Eds.), Sedimentation in Oblique Slip Mobile Zones. Special Publications of the International Association of Sedimentologists, vol. 4, pp. 27–41.

Royden, L.H., 1985. The Vienna Basin: a thin-skinned pull-apart basin. In: Biddle, K.T., Christie-Blick, N. (Eds.), Strike-Slip Deformation, Sedimentation, Basin Formation. Society of Economic Paleontologists and Mineralogists, Special Publication, vol. 37, pp. 319–338.

Sauer, R., Seifert, P., Wessely, G., 1992. Guidebook to excursions in the Vienna Basin and the adjacent Alpine–Carpathian thrust belt in Austria. Mitteilungen der Österreichischen Geologischen Gesellschaft 85, 1–264.

Schreurs, G., Colleta, B., 1998. Analogue modeling of faulting in zones of continental transpression and transtension. In: Holdsworth, R.E., Strachan, R.A., Dewey, J.F. (Eds.), Continental Transpressional and Transtensional Tectonics. Geological Society of London, Special Publications, vol. 135, pp. 59–79.

Schreurs, G., Buiter, S.J.H., Boutelier, D., Corti, G., Costa, E., Cruden, A., Daniel, J.-M., Hoth, S., Koyi, H., Kukowski, N., Lohrmann, J., Ravaglia, A., Schlische, R.W., Withjack, M.O., Yamada, Y., Cavozzi, C., Delventisette, C., Elder Brady, J.A., Hoffmann-Rothe, A., Mengus, J.-M., Montanari, D., Nilforoushan, F., 2006. Analogue benchmarks of shortening and extension experiments. In: Buiter, S.J.H., Schreurs, G. (Eds.), Analogue and Numerical Modelling of Crustal-Scale Processes. Geological Society of London, Special Publications, vol. 253, pp. 1–27.

Schubert, C., 1982. Origin of Cariaco basin, South Caribbean Sea. Marine Geology 47, 345–360.

Sims, D., Ferrill, D.A., Stamatakos, J.A., 1999. Role of a ductile decollement in the development of pull-apart basins: experimental results and natural examples. Journal of Structural Geology 21, 533–554.

Smit, J., Brun, J.P., Fort, X., Cloetingh, S., Ben-Avraham, Z., 2008. Salt tectonics in pull-apart basins with application to the Dead Sea Basin. Tectonophysics 449 (1–4), 1–16.

Sylvester, A.G., 1988. Strike-slip faults. Geological Society of America Bulletin 100, 1666–1703.

Tron, V., Brun, J.P., 1991. Experiments on oblique rifting in brittle–ductile systems. Tectonophysics 188, 71–84.

Wdowinski, S., Bock, Y., Baer, G., Prawirodirdjo, L., Bechor, N., Naaman, S., Knafo, R., Forrai, Y., Melzer, Y., 2004. GPS measurements of current crustal movements along the Dead Sea Fault. Journal of Geophysical Research 109, B05403.

Weijermars, R., 1986. Flow behaviour and physical chemistry of bouncing putties and related polymers in view of tectonic laboratory applications. Tectonophysics 124, 325–358.

Wesnousky, S.G., 1988. Seismological and structural evolution of strike-slip faults. Nature 335, 340–343.

Whitehouse, P.S., 2005. Fault and Fracture Development in Extensionally Reactivated Fault Systems. PhD thesis, University of London (unpublished), 596 pp.

Wood, R., Pettinga, J.R., Bannister, S., Lamarche, G., McMorran, T., 1994. Structure of the Hanmer strike-slip basin, Hope fault, New Zealand. Geological Society of America Bulletin 106, 1459–1473.

Woodcock, N.H., Fischer, M., 1986. Strike-slip duplexes. Journal of Structural Geology 8, 725–735.

Zhang, P., Burchfiel, B.C., 1989. Extinction of pull-apart basins. Geology 17, 814–817.